Modern Pathology (2019) 32:1521–1535
https://doi.org/10.1038/s41379-019-0283-z

ARTICLE

Xp11 translocation renal cell carcinoma and clear cell renal cell carcinoma with TFE3 strong positive immunostaining: morphology, immunohistochemistry, and FISH analysis

Bo Yang[1] · Haoqing Duan[2] · Wenfeng Cao[1] · Yuhong Guo[1] · Yanxue Liu[1] · Lin Sun[1] · Jingyi Zhang[1] · Yan Sun[1] · Yongjie Ma[3]

Received: 10 January 2019 / Revised: 12 April 2019 / Accepted: 15 April 2019 / Published online: 7 June 2019

Abstract

TFE3 is accepted as a good marker for the diagnosis of Xp11 translocation renal cell carcinoma. However, the significance of TFE3 in other types of renal cell carcinomas remains unclear. We examined the expression of TFE3 using immunohistochemistry by automated Ventana BenchMark XT system in 1818 consecutive renal cell carcinomas and verified the strong positive cases with *TFE3* break-apart fluorescence in situ hybridization and RNA sequencing. Among the 27 renal cell carcinomas with TFE3 strong positive immunostaining, 20 cases were diagnosed as Xp11 translocation renal cell carcinoma, and seven cases were diagnosed as clear cell renal cell carcinoma. We further analyzed the morphology, clinicopathological features, and immunohistochemistry markers (CK7, CD117, CD10, P504s, vimentin, CA-IX, AE1/AE3, EMA, HMB45, Melan-A, and cathepsin K) of them. Pale to eosinophilic flocculent cytoplasm and psammomatous calcification were seen only in Xp11 translocation renal cell carcinomas ($P < 0.05$). Tumor necrosis occurred in all four cases of Xp11 translocation renal cell carcinomas with pT3a stage, which had local recurrence and distant metastasis (two of them died) within 3 years. The expressions of Vimentin, CA-IX, AE1/AE3, and EMA were significantly different between them ($P < 0.05$). CA-IX was diffusely strong positive in clear cell renal cell carcinomas but negative or focally mild positive in Xp11 translocation renal cell carcinomas. Our study first demonstrates that a very small minority (0.4%) of clear cell renal cell carcinomas with TFE3 strong positive immunostaining, which points out a potential pitfall in diagnosis of Xp11 translocation renal cell carcinomas by TFE3 immunohistochemistry. CA-IX is a good marker to distinguish clear cell renal cell carcinoma with TFE3 strong positive immunostaining from Xp11 translocation renal cell carcinoma. Tumor necrosis could be a potential factor relevant to pT3a stage, which may be a high-risk factor for the patients with Xp11 translocation renal cell carcinomas.

Introduction

Xp11 translocation renal cell carcinoma is a rare renal cell carcinoma subtype harboring *TFE3* translocation, which was officially recognized as a distinct entity in the 2004 World Health Organization (WHO) Classification of Renal

These authors contributed equally: Bo Yang, Hao-qing Duan

Supplementary information The online version of this article (https://doi.org/10.1038/s41379-019-0283-z) contains supplementary material, which is available to authorized users.

✉ Yan Sun
sunyan@tjmuch.com

✉ Yongjie Ma
mayongjie@tjmuch.com

[1] Department of Pathology, Tianjin Medical University Cancer Institute and Hospital, National Clinical Research Center for Cancer, Key Laboratory of Cancer Prevention and Therapy, Tianjin, Tianjin's Clinical Research Center for Cancer, Tianjin, China

[2] Clinical Laboratory Center, Institute of Hematology and Blood Diseases Hospital, Chinese Academy of Medical Sciences and Peking Union Medical College, Tianjin, China

[3] Department of tumor cell biology, Tianjin Medical University Cancer Institute and Hospital, National Clinical Research Center for Cancer, Key Laboratory of Cancer Prevention and Therapy, Tianjin, Tianjin's Clinical Research Center for Cancer, Tianjin, China

Tumors at first time, and grouped into MiT family translocation renal cell carcinomas together with t (6;11) translocation renal cell carcinomas in the latest 2016 WHO Classification [1, 2]. Xp11 translocation renal cell carcinomas account for the majority of pediatric renal cell carcinoma and about 1–4% of adult renal cell carcinoma [3–5]. The outcome of Xp11 translocation renal cell carcinomas is similar to clear cell renal cell carcinomas, with increased age and advanced stage being adverse prognostic factors [3, 6, 7]. The reported known TFE3 fusion partners include *ASPSCR1* (*ASPL*), *PRCC*, *SFPQ1* (*PSF*), *NONO* (*p54nrb*), *CLTC*, *LUC7L3*, *KHSRP*, *PARP14*, *DVL2*, *RBM10*, *MED15*, *GRIPAP1*, *ARID1B*, *MATR3*, and *FUBP1*, and different gene fusions demonstrate unique morphologic patterns with overlapping among different genotypes of them simultaneously, and the most common morphology is that of Xp11 translocation renal cell carcinomas with clear cells, papillary architecture, and psammoma bodies [8–19].

TFE3 break-apart fluorescence in situ hybridization (FISH) assay is currently the gold standard to identify *TFE3* rearrangement on formalin-fixed and paraffin-embedded tissue sections [20]. Immunohistochemistry staining with the antibody from C-terminal portion of TFE3 is the most commonly used assay in the diagnosis of Xp11 translocation renal cell carcinomas with strong nuclear TFE3 immunoreactivity [21]. TFE3 immunohistochemistry staining was usually performed with manual immunohistochemistry detection and Dako Link Plus staining system in the previous studies, but the concordance rates of TFE3 immunohistochemistry staining and FISH analysis were 0–83% [20, 22–25]. The huge difference of concordance rates mainly resulted from different fixation time, technical methods, and scoring systems. Considering immunohistochemistry staining is the most convenient strategy in the clinical diagnosis, especially in the developing countries, an efficient and stable detection system is needed for TFE3 immunohistochemistry staining.

In this study, we performed TFE3 immunohistochemistry staining by an automated Ventana BenchMark XT system in 1818 consecutive renal cell carcinomas and verified the strong positive cases with *TFE3* break-apart FISH assay and RNA sequencing. Among the 27 cases renal cell carcinomas with TFE3 strong positive immunostaining, 20 renal cell carcinomas were diagnosed as Xp11 translocation renal cell carcinomas, and seven cases were diagnosed as clear cell renal cell carcinomas. We not only report the ratio of Xp11 translocation renal cell carcinoma in Chinese patients with renal cell carcinoma through this large-scale study, but also indicate a very small minority of clear cell renal cell carcinomas with strong nuclear immunostaining of TFE3. We further compared the morphology, clinicopathological features, and immunohistochemistry patterns between 20 Xp11 translocation renal cell carcinomas and seven clear cell renal cell carcinomas in order to supply some hints to avoid the potential pitfalls in the diagnosis of Xp11 translocation renal cell carcinomas.

Materials and methods

Case selection

We collected the 1818 consecutive renal cell carcinomas, which underwent partial or radical nephrectomy and had the immunohistochemistry staining of a panel (PAX8, CD10, carbonic anhydrase IX/CA-IX, Vimentin, CK7, CD117, P504s, and TFE3) at Tianjin Medical University Cancer Institute & Hospital from January 2013 to December 2017. The hematoxylin & eosin (H&E) and immunohistochemistry staining slides were reviewed independently by experienced pathologists (B.Y. and W.C). Finally, 1604 (88.2%), 98 (5.4%), 80 (4.4%), 20 (1.1%), and 16 cases (0.9%) were diagnosed as clear cell renal cell carcinoma, papillary renal cell carcinoma, chromophobe renal cell carcinoma, Xp11 translocation renal cell carcinoma and other subtypes of renal cell carcinomas, respectively. The data were collected including clinicopathological features, treatments, and follow-up information (all patients were followed until April 2018). This study was approved by the Ethical Review Committee of Tianjin Medical University Cancer Institute & Hospital.

Immunohistochemistry

Tumor tissues were fixed in 10% formalin and embedded in paraffin. The 4-μm-thick whole sections were performed immunohistochemistry staining with an automated Ventana BenchMark XT system (Roche, Ventana Medical Systems Inc., Tucson) for the following antibodies: TFE3 (SC-5958, 1:300; Santa Cruz, CA), CathepsinK (3F9, 1:300; Abcam), CA-IX (ab1508, 1:1000; Abcam), HMB45 (prediluted; MXB Biotechnologies, Fuzhou, China), Melan-A (A103/M2–72, prediluted; MXB Biotechnologies), PAX8 (4H7B3, 1:100; ProteinTech Group, Rosemont, IL), CD10 (56C6, prediluted; MXB Biotechnologies), Vimentin (V9, prediluted; MXB Biotechnologies), CK7 (OV-TL12/30, prediluted; MXB Biotechnologies), P504s (13H4, prediluted; MXB Biotechnologies), CD117 (YR145, prediluted; MXB Biotechnologies), EMA (E29, prediluted; MXB Biotechnologies), and AE1/AE3 (prediluted; MXB Biotechnologies). Positive and negative controls yielded appropriate results for each antibody.

Immunoreactivity was evaluated in a semiquantitative manner based on both labeling intensity and the percentage of immunopositive tumor cells for all antibodies. The score was calculated by multiplying the staining intensity (0 = no

staining, 1 = mild staining, 2 = moderate staining, and 3 = strong staining) by the percentage of immunoreactive tumor cells (0–100). The immunostaining result was considered to be negative (0) when the score was <25; weak positive (1+) when the score was 26–100; moderate positive (2+) when the score was 101–200; or strong positive (3+) when the score was 201–300.

FISH

The commercial dual-color break-apart FISH probes (*TFE3* Break Apart FISH Probe Kit) were bought from ShaoxingJinlu Biotechnology (Shaoxing, Zhejiang China). The clones CH17-465H20 (chrX:49330483-49679869) and CH17-404G18 (chrX:49102802-49318218) (total 470 kbp) located telomeric to the *TFE3* gene were labeled with 5-ROX dUTP (red), and the clones CH17-340M11 (chrX:48562070-48773968) and CH17-28J19 (chrX:48803374-49034608) (total 580 kbp) located centromeric to the *TFE3* gene were labeled with 5-fluorescein dUTP (green).

FISH assay was performed on all of the renal cell carcinomas with TFE3 strong positive immunostaining as described previously [26]. The 4-μm-thick tissue sections from formalin-fixed and paraffin-embedded tissue blocks were transferred to positively charged slides and baked at 60 °C for 2 h. These slides were deparaffinized by three 10-min xylene washes and two 5-min 100%-ethanol washes. The slides were incubated in 4 mg/mL pepsin solution (in 0.2 N HCl, pH 1.0) at 37 °C for 30 min. A 10-μL *TFE3* probe mixture (probe: hybridization buffer: purified H_2O= 1:7:2) was added to every slide and sealed under a coverslip with rubber cement. The slides were then incubated at 85 °C for 5 min to co-denature with the probes, followed by hybridization in a humidified chamber (HYBrite, Vysis, Downers Grove, IL, USA) at 37 °C overnight. After coverslips were removed, the slides were soon immersed in posthybridization buffer (2 × SSC with 0.3% NP40) at 73 °C for 2 min, followed by a 2-min wash in 2 × SSC/ 0.1% NP40 at room temperature. Finally, the slides were air dried, counterstained with 20 μL of 4′,6-diamidino-2-phenylindole (DAPI) II reagent (Vysis) and coverslips were applied.

Fluorescence signals were analyzed using a Nikon Eclipse 90i fluorescence microscope (Nikon, Tokyo, Japan) equipped with an appropriate filter set. Signals were considered to be split when the green and red signals were separated by a distance ≥2 signal diameters. One hundred non-overlapping nuclei, which were clearly identified and contained unequivocal signals, were counted for each case. On the basis of the generally accepted guidelines used by all other commercially available break-apart FISH assays and developed *TFE3* break-apart FISH assays, a positive result was reported when >10% of the tumor nuclei showed the split-signal pattern [19, 20].

RNA sequencing

Seven cases of clear cell renal cell carcinomas with TFE3 strong positive immunostaining were analyzed by RNA sequencing from Nanjing Geneseeq Technology Inc. (Nanjing, Jiangsu China). Total RNA from formalin-fixed paraffin-embedded samples was extracted using RNeasy FFPE kit (QIAGEN). Ribosomal RNA was depleted using RNase H followed by library preparation using KAPA Stranded RNA-seq Kit with RiboErase (HMR) (KAPA Biosystems). Library concentration was determined by KAPA Library Quantification Kit (KAPA Biosystems), and library quality was accessed by Agilent High Sensitivity DNA kit on Bioanalyzer 2100 (Agilent Technologies), which was then sequenced on Illumina HiSeq NGS platforms (Illumina).

Three tools were applied for fusion detection of RNA sequencing data. FusionCatcher (verison 0.99.4e) was used with parameters (–aligners blat, otherwise default parameter) which uses Bowtie aligner to perform both transcriptome and genome mapping and then uses BLAT aligner to further map unmapped reads and count fusion supporting evidence. The other two tools namely Factera and Socrates (https://github.com/jibsch/Socrates) were both executed using default parameters. Specially, Socrates takes the modified BAM file, which converted hard-clip in original BAM into soft-clip to improve the fusion detection performance. The combined fusion results from all tools were manually reviewed on Integrative Genomics Viewer for confirmation.

Statistics

Results were analyzed using SPSS 19.0 software (SPSS Inc., Chicago, IL, USA). Relationships between qualitative variables were investigated using two tailed Chi-Square test or Fisher's exact test, and quantitative variables were analyzed by *t*-test. Cumulative survival time was calculated by the Kaplan–Meier method and analyzed by the log-rank test. *P*-value of less than 0.05 was considered significant.

Results

TFE3 immunohistochemistry, FISH, and RNA sequencing

The immunohistochemistry staining for TFE3 can be evaluated in all of the 1818 renal cell carcinomas. There was no TFE3 staining in paraneoplastic normal renal tubular epithelium with a clean background. TFE3 was strong positive in the tumor nuclei of 27 renal cell carcinomas, including all of the 20 Xp11 translocation renal cell

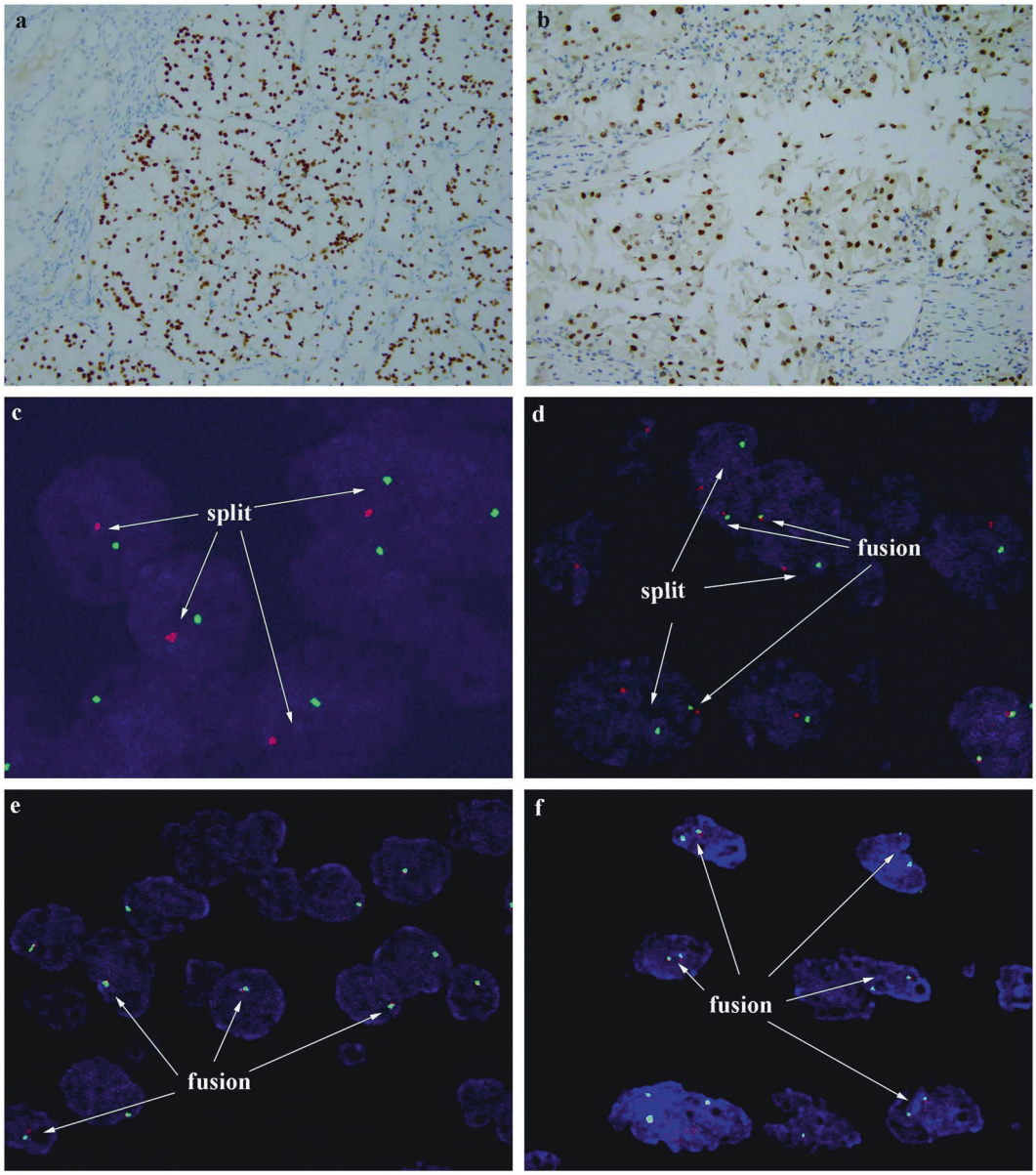

Fig. 1 Immunohistochemistry staining and FISH analysis for TFE3 between 20 Xp11 translocation renal cell carcinomas and seven clear cell renal cell carcinomas. **a** Xp11 translocation renal cell carcinoma with TFE3 strong positive immunostaining, ×200. **b** Clear cell renal cell carcinoma with TFE3 strong positive immunostaining, ×200. **c** Male of Xp11 translocation renal cell carcinoma showed one red and one green signal, and **d** female of Xp11 translocation renal cell carcinoma showed one red, one green, and one fusion signal. **e** Male of clear cell renal cell carcinoma showed one fusion signal, and **f** female of clear cell renal cell carcinoma showed two fusion signals

carcinomas (Fig. 1a) and seven cases of clear cell renal cell carcinomas (Fig. 1b & Supplementary Fig. S1). Moreover, 13 cases of clear cell renal cell carcinomas showed focally mild or moderate positive (1+) immunostaining for TFE3 (Supplementary Fig. S2). In addition, TFE3 was negative in all of the papillary renal cell carcinomas, chromophobe renal cell carcinomas and other subtypes of renal cell carcinomas.

We further performed *TFE3* break-apart FISH analysis for 27 renal cell carcinomas with TFE3 strong positive immunostaining. Since *TFE3* is located in X chromosome, the positive signal pattern differs between male and female patients: males with *TFE3* translocation showed one red and one green signal (Fig. 1c), whereas females showed one red, one green, and one fusion (yellow) signal (Fig. 1d). The negative signal pattern was one fusion (yellow) signal for males (Fig. 1e) and two fusion (yellow) signals for females (Fig. 1f). All of 20 cases of Xp11 translocation renal cell carcinomas showed *TFE3* break-apart positive results, whereas all of seven cases of clear cell renal cell carcinomas

demonstrated *TFE3* break-apart negative results. In addition, no *TFE3* amplification was detected.

None of *TFE3*-related gene fusions were found in all of the seven clear cell renal cell carcinomas by RNA sequencing, but one unrelated gene fusion, *SCNN1A-TNFRSF1A*, was identified in only one case (case 27) (Supplementary Fig. S3).

Morphologic features of 20 Xp11 translocation renal cell carcinomas and seven clear cell renal cell carcinomas

The morphologic features of the 27 renal cell carcinomas with TFE3 strong positive immunostaining are shown in Table 1. The following histopathologic features were only detected in Xp11 translocation renal cell carcinomas: cystic architecture similar to multilocular cystic renal neoplasm of low malignant potential (Fig. 2a), high columnar cells and nuclei toward the luminal surface (secretory endometrioid, Fig. 2b), resembling collecting duct carcinoma architecture (Fig. 2c), entrapped benign renal tubules (Fig. 2d), psammomatous calcification (Fig. 2e), foamy histiocytes (Fig. 2f), only eosinophilic cytoplasm (Fig. 3a), pale to eosinophilic flocculent cytoplasm (Fig. 3b), cytoplasmic melanin pigment (Fig. 3c), nuclear pseudoinclusions (Fig. 3d), cytoplasmic vacuolization (Fig. 3e), cytoplasmic eosinophilic granular bodies (Fig. 3f). On the other hand, pseudopapillary architecture (Fig. 4a), extreme nuclear pleomorphism (Fig. 4b) and rhabdoid differentiation (Fig. 4c) appeared only in clear cell renal cell carcinomas. The comparison of detailed morphologic findings between 20 Xp11 translocation renal cell carcinomas and seven clear cell renal cell carcinomas are presented in Table 2. There were significant differences in the following features between the two groups: pale to eosinophilic flocculent cytoplasm ($P = 0.046$), psammomatous calcification ($P = 0.018$), pseudopapillary architecture ($P = 0.013$), and extreme nuclear pleomorphism ($P = 0.013$). Moreover, although necrosis was observed in both groups, it was more frequent in clear cell renal cell carcinomas than Xp11 translocation renal cell carcinomas ($P = 0.013$, Fig. 4d). However, the alveolar/nested, papillary, solid, trabecular architectures and only clear cytoplasm as well as clear and eosinophilic cytoplasm were seen in both Xp11 translocation renal cell carcinomas and clear cell renal cell carcinomas, not showing the significant difference ($P > 0.05$).

Clinicopathological features of 20 Xp11 translocation renal cell carcinomas and seven clear cell renal cell carcinomas

The clinicopathological features of the 27 renal cell carcinomas with TFE3 strong positive immunostaining are shown in Table 1. Tumor necrosis occurred in all four cases of Xp11 translocation renal cell carcinomas with pT3a stage, but it never occurred in other cases of Xp11 translocation renal cell carcinomas with non-pT3a stage. However, tumor necrosis occurred in five cases of clear cell renal cell carcinomas including one case of pT1a stage, one case of pT1b stage, and three cases of pT3a stage. The comparison of clinicopathological features between 20 Xp11 translocation renal cell carcinomas and seven clear cell renal cell carcinomas are showed in Table 3. The results displayed that the mean age of patients, tumor size, and nuclear WHO/International Society of Urological Pathology (ISUP) grade were significantly different between 20 Xp11 translocation renal cell carcinomas and seven clear cell renal cell carcinomas ($P < 0.05$), but there was no significant difference in the sex ratio and pTNM stage (according to the 2018 American Joint Committee on Cancer TNM staging system) between them ($P > 0.05$). Compared with clear cell renal cell carcinomas, Xp11 translocation renal cell carcinomas were younger in age of patients, smaller in tumor size and lower in WHO/ISUP grading.

Table 1 shows the follow-up data for all 27 patients (range, 6–47 months; mean, 29 months), and five of them were treated with biotherapy by dendritic cell vaccines after operation. After the initial resection, 21 patients were alive with no evidence of disease, two patients were alive with distant metastasis, one patient died of myocardial infarction 14 months after operation, and three patients died of distant metastasis 32 months, 36 months, and 14 months after operation respectively. Within 3 years, all four patients of Xp11 translocation renal cell carcinomas with pT3a stage had local recurrence and distant metastasis, and two of them died. Nevertheless, among all three cases of clear cell renal cell carcinomas with pT3a stage, except one patient died from brain metastasis 13 months after operation, the other two patients had no evidence of disease with 42 and 43 months, respectively. Kaplan–Meier analysis showed that there was no significant difference in overall survival and disease-free survival between 20 Xp11 translocation renal cell carcinomas and seven clear cell renal cell carcinomas ($P = 0.861$ and $P = 0.670$, respectively; Supplementary Fig. S4). The mean overall survival times were 41.5 months and 42.3 months, and the mean disease-free survival times were 36.7 months and 42.1 months, for patients with Xp11 translocation renal cell carcinomas and clear cell renal cell carcinomas, respectively.

Immunohistochemistry profiles of the 20 Xp11 translocation renal cell carcinomas and 7 clear cell renal cell carcinomas

The immunohistochemistry profiles of 27 renal cell carcinomas with TFE3 strong positive immunostaining are

Table 1 Morphologic and clinicopathological features of 27 renal cell carcinomas with strong positive immunostaining for TFE3

Case	Age	Sex	Diagnosis	Size (cm)	Grade (ISUP)	Stage (pTNM)	Morphologic features	Follow-up (mo)
1	28	F	Xp11 TRCC	3.5	3	pT1aNxMx	Alveolar or nested, solid architecture by nodule-in-nodule like pattern; clear (alveolar or nested) and eosinophilic (solid) cytoplasm; non-psammomatous calcification	44, NED
2	21	M	Xp11 TRCC	3.5	3	pT1aNxMx	Alveolar or nested, papillary architecture, voluminous clear and eosinophilic cytoplasm, psammomatous calcification, foamy histiocytes	43, NED; seven rounds of BTDCV after operation
3	36	M	Xp11 TRCC	4.5	3	pT1bN1Mx	Alveolar or nested, papillary architecture; voluminous clear and eosinophilic cytoplasm; psammomatous calcification	41, NED; Cryosurgery of argon and helium of retroperitoneal lymph nodes one month after operation
4	13	M	Xp11 TRCC	4.8	3	pT3aN1Mx	Alveolar or nested, papillary, solid architecture; pale to eosinophilic flocullent cytoplasm; cytoplasmic eosinophilic granular bodies; necrosis; renal vein invasion	32, DOD; Lung,bone, mediastinal lymph nodes metastasis 14 months after operation
5	59	F	Xp11 TRCC	7.0	2	pT1bNxMx	Alveolar or nested architecture by hyalinized and calcified vascular septa; pale to eosinophilic flocullent cytoplasm	41, NED; three rounds of BTDCV after operation
6	48	F	Xp11 TRCC	3.0	2	pT1aNxMx	Alveolar or nested architecture; pale to eosinophilic flocullent cytoplasm; psammomatous calcification	38, NED
7	34	M	Xp11 TRCC	5.0	2	pT3aNxMx	Alveolar or nested architecture; voluminous clear and occasionally eosinophilic cytoplasm; psammomatous calcification; necrosis; spread to peripheral perinephric fat	36, DOD; four rounds of BTDCV after operation; Lung,bone, mediastinal lymph nodes metastasis 11 months after operation
8	63	M	Xp11 TRCC	2.0	2	pT1aNxMx	Papillary architecture; voluminous eosinophilic cytoplasm; foamy histiocytes	34, NED; three rounds of BTDCV after operation
9	32	F	Xp11 TRCC	6.0	2	pT3aNxMx	Alveolar or nested,trabecular; pale to eosinophilic flocullent cytoplasm; necrosis; renal vein invasion	34, AWD; Recurred in operative region,lung and cervical vertebrae metastasis 6 months after operation
10	40	F	Xp11 TRCC	4.0	2	pT1bNxMx	Alveolar or nested architecture; voluminous clear cytoplasm; high columnar cells and nuclei toward the luminal surface (secretory endometrioid); psammomatous calcification; foamy histiocytes	31, NED; two rounds of BTDCV after operation
11	47	M	Xp11 TRCC	2.2	2	pT1aNxMx	Papillary architecture; voluminous pale to eosinophilic flocullent cytoplasm; psammomatous calcification	30, NED
12	34	F	Xp11 TRCC	5.0	2	pT1bNxMx	Alveolar or nested architecture by hyalinized vascular septa; clear cytoplasm	26, NED
13	21	M	Xp11 TRCC	6.0	3	pT3aN1Mx	Papillary, glandular, tubular architecture resembling collecting duct carcinoma; pale to eosinophilic flocullent cytoplasm; necrosis; psammomatous calcification; renal vein, sinus fat, pelvis invasion	25, AWD; lung and bone metastasis 6 and 9 months after operation, respectively
14	24	F	Xp11 TRCC	5.0	3	pT1bNxMx	Alveolar or nested, solid, papillary architecture; clear (alveolar, nested, solid) and eosinophilic (papillary) cytoplasm; psammomatous calcification	23, NED
15	53	M	Xp11 TRCC	7.0	3	pT1bNxMx		21, NED

Table 1 (continued)

Case	Age	Sex	Diagnosis	Size (cm)	Grade (ISUP)	Stage (pTNM)	Morphologic features	Follow-up (mo)
							Papillary, nested, solid, cystic architecture; voluminous eosinophilic cytoplasm; psammomatous calcification; foamy histiocytes	
16	52	M	Xp11 TRCC	2.8	2	pT1aNxMx	Alveolar or nested,papillary architecture; voluminous pale to eosinophilic flocullent cytoplasm; psammomatous calcification	21, NED
17	61	F	Xp11 TRCC	3.5	3	pT1aNxMx	Papillary architecture; voluminous eosinophilic and occasionally clear cytoplasm; foamy histiocytes	20, NED
18	53	F	Xp11 TRCC	1.0	2	pT1aNxMx	Alveolar or nested architecture; voluminous pale to eosinophilic flocullent cytoplasm; cytoplasmic melanin pigment; entrapped benign renal tubules	14, DUD (death from myocardial infarction)
19	18	M	Xp11 TRCC	5.0	3	pT1bNxMx	Alveolar or nested architecture; voluminous eosinophilic cytoplasm; cytoplasmic melanin pigment; nuclear pseudoinclusions; cytoplasmic vacuolization	10, NED
20	47	F	Xp11 TRCC	6.0	1	pT1bNxMx	Predominant cystic and occasionally nested architecture similar to multilocular cystic renal neoplasm of low malignant potential; clear cytoplasm; non-psammomatous calcification	6, NED
21	45	M	CCRCC	10.0	2	pT2aNxMx	Alveolar or nested architecture; clear cytoplasm	47, NED
22	61	M	CCRCC	10.0	4	pT3aNxMx	Alveolar or nested architecture; voluminous clear and eosinophilic cytoplasm; extreme nuclear pleomorphism; necrosis; spread to peripheral perinephric fat	43, NED
23	55	M	CCRCC	7.5	4	pT3aN0Mx	Alveolar or nested architecture; voluminous clear and occasionally eosinophilic cytoplasm, extreme nuclear pleomorphism; necrosis; renal vein invasion	42, NED
24	53	F	CCRCC	8.0	4	pT3aN1Mx	Alveolar or nested, solid architecture; voluminous clear and occasionally eosinophilic cytoplasm; rhabdoid differentiation; necrosis; renal vein invasion	14, DOD; Lung,bone,brain (death from hemorrhage and rupture of tumor) metastasis 13 months after operation
25	68	M	CCRCC	1.8	2	pT1aNxMx	Alveolar or nested architecture; clear cytoplasm	25, NED
26	48	M	CCRCC	3.5	3	pT1aNxMx	Alveolar or nested, pseudopapillary architecture; voluminous clear and occasionally eosinophilic cytoplasm; necrosis	24, NED
27	54	M	CCRCC	6.0	3	pT1bNxMx	Alveolar or nested, trabecular, pseudopapillary architecture; voluminous eosinophilic and occasionally clear cytoplasm; necrosis	14, NED

Xp11 TRCC Xp11 translocation renal cell carcinoma, *CCRCC* clear cell renal cell carcinoma, *ISUP* International Society of Urological Pathology, *DOD* died of disease, *NED* no evidence of disease, *AWD* alive with disease, *DUD* died of causes unrelated disease, *BTDCV* biotherapy by dendritic cell vaccines

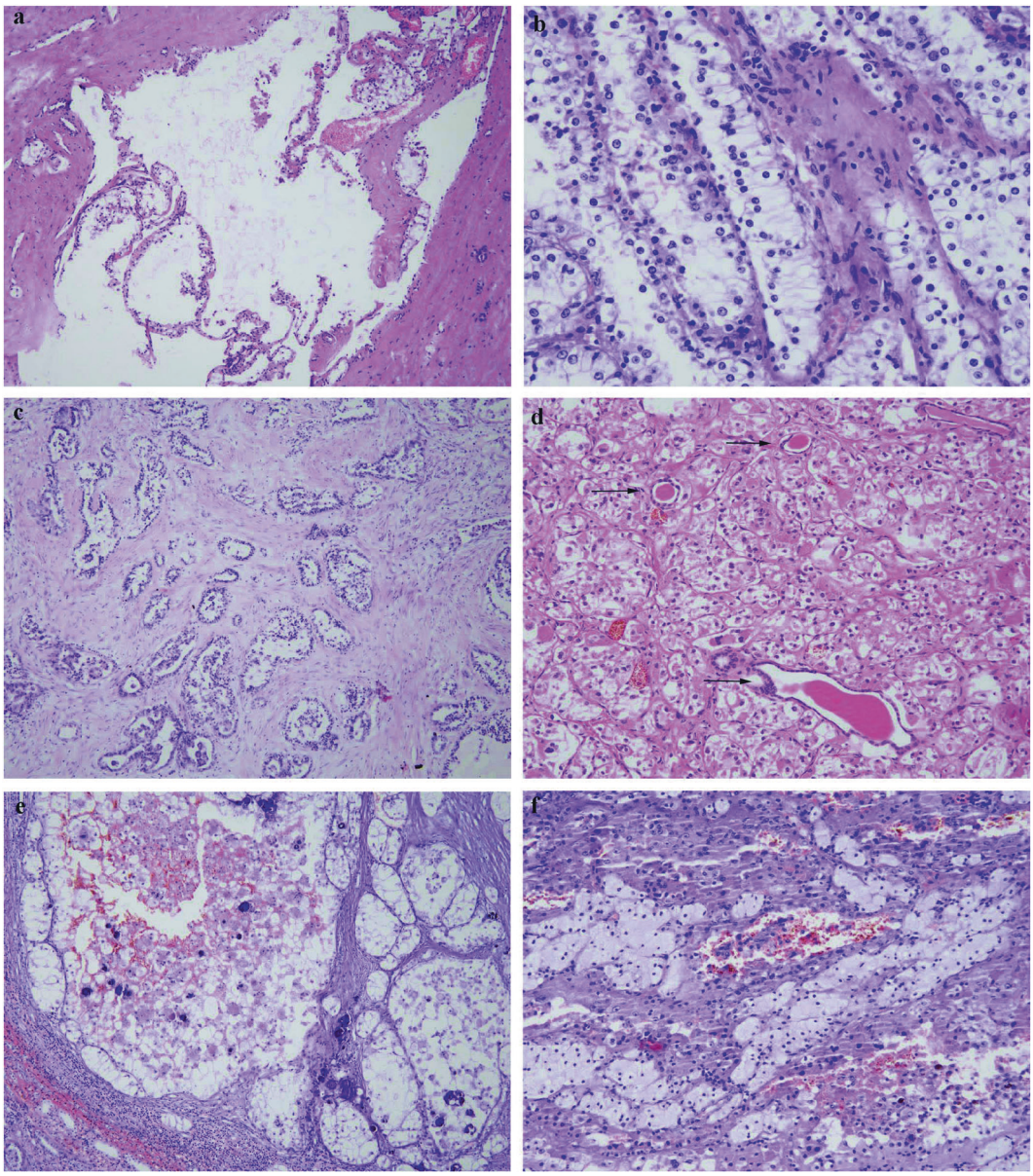

Fig. 2 Some histopathologic features were only detected in Xp11 translocation renal cell carcinomas, including **a** cystic architecture similar to multilocular cystic renal neoplasm of low malignant potential, H&E, ×200; **b** high columnar cells and nuclei toward the luminal surface mimicked secretory endometrioid architecture, H&E, ×400; **c** resembling collecting duct carcinoma architecture, H&E, ×100; **d** entrapped benign renal tubules, H&E, ×200; **e** psammomatous calcification, H&E, ×100; **f** foamy histiocytes, H&E, ×200

shown in Supplementary Table S1, and the comparison of immunohistochemistry findings between 20 Xp11 translocation renal cell carcinomas and seven clear cell renal cell carcinomas are summarized in Table 4. All of the 27 renal cell carcinomas exhibited moderate positive (2+) or strong positive (3+) staining for PAX8 (Fig. 5a). P504s, Vimentin, AE1/AE3, and CA-IX were positive in 19 (95%), 10 (50%), 10 (50%), and 2 (10%) cases of 20 Xp11 translocation renal cell carcinomas, respectively; whereas they were all positive in seven clear cell renal cell carcinomas. The positive ratio of Vimentin ($P = 0.018$), AE1/AE3 ($P = 0.018$), and CA-IX ($P < 0.001$) in clear cell renal cell carcinomas was significantly higher than that in Xp11 translocation renal cell carcinomas. In addition, CK7 (Fig. 5b), CD117 (Fig. 5c), HMB45 (Fig. 5d), Melan-A (Fig. 5e), and CathepsinK (Fig. 5f) were positive in 3 (15%), 1 (5%,), 2 (10%), 3 (15%,), and 6 (30%) of 20 Xp11 translocation renal cell carcinomas, respectively; whereas they were all negative in seven clear cell renal cell carcinomas. The positive ratio of EMA was significantly lower in Xp11 translocation renal cell carcinomas (4/20, 20%) than that (5/7, 71%) in clear cell renal cell carcinomas ($P = 0.013$). There was no

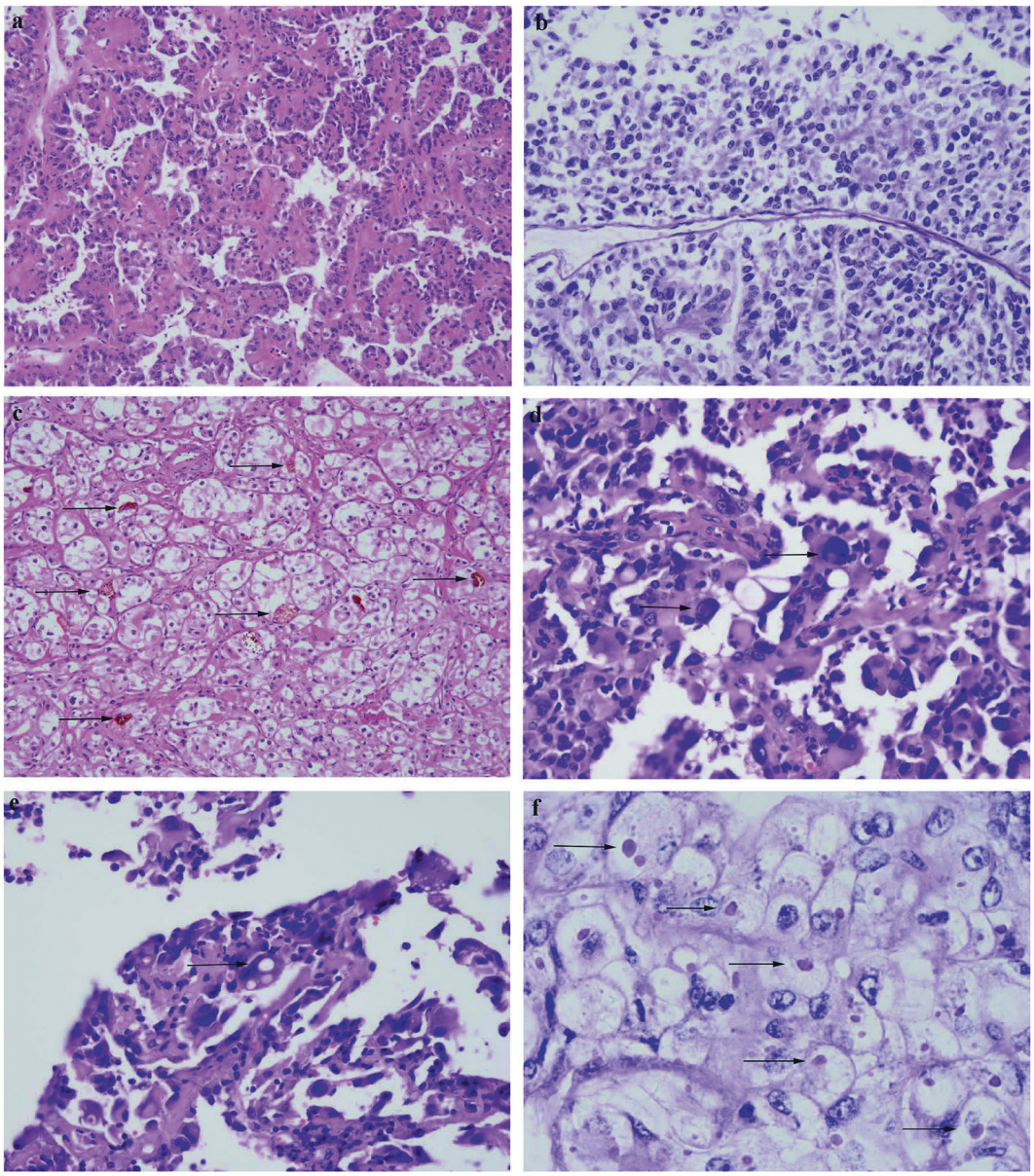

Fig. 3 The other histopathologic features were only detected in Xp11 translocation renal cell carcinomas, including **a** only eosinophilic cytoplasm, H&E, ×200; **b** pale to eosinophilic flocculent cytoplasm cells, H&E, ×400; **c** cytoplasmic melanin pigment, H&E, ×200; **d** nuclear pseudoinclusions, H&E, ×400; **e** cytoplasmic vacuolization, H&E, ×400; **f** cytoplasmic eosinophilic granular bodies, H&E, ×1000

significant difference of CD10 expression between Xp11 translocation renal cell carcinomas (13/20, 65%) and clear cell renal cell carcinomas (6/7, 86%). Besides positive ratio, there were some different positive staining patterns for some markers between the two kinds of renal cell carcinoma groups. CA-IX (Fig. 6a), AE1/AE3 (Fig. 6b), and EMA (Fig. 6c) were only focally mild or moderate positive staining in Xp11 translocation renal cell carcinomas except for two cases of AE1/AE3 and 1 case of EMA with diffusely strong positive staining, but they were all diffusely strong positive staining in clear cell renal cell carcinomas (Fig. 6d-f).

Discussion

In this study, we reported the ratio of Xp11 translocation renal cell carcinomas was 1.1% in the consecutive 1818 renal cell carcinomas from our cancer center between 2013 and 2017, which is similar to the ratio of other studies [5, 6]. Only one case is a child (13 years old) in our Xp11 translocation renal cell carcinomas, which is consistent with the viewpoint made by Argani and colleagues that *TFE3*-rearranged renal cell carcinomas from adults are likely to represent a quantitatively larger number of tumors as a whole than those from children because renal cell

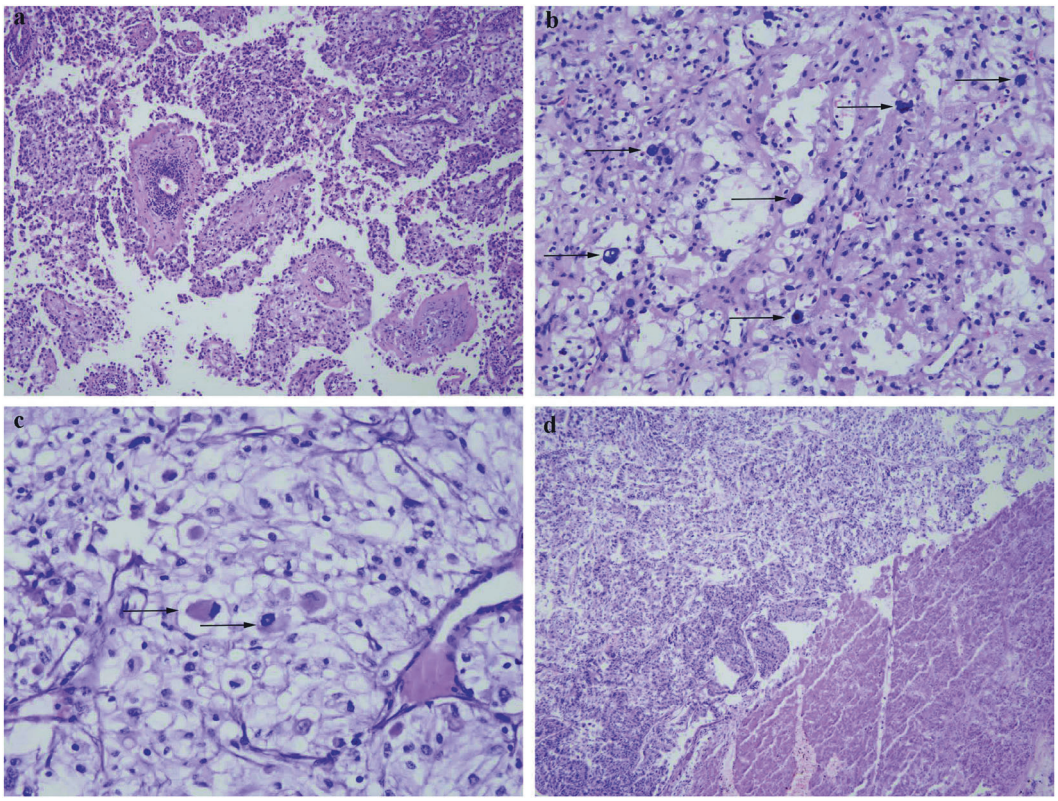

Fig. 4 Some histopathologic features were only found in clear cell renal cell carcinomas, including **a** pseudopapillary architecture, H&E, ×100; **b** extreme nuclear pleomorphism, H&E, ×200; **c** rhabdoid differentiation, H&E, ×400. **d** Necrosis in Xp11 translocation renal cell carcinoma, H&E, ×100

carcinomas are far more common in adults relative to children [27]. As far as we know, our study is the first large-scale study about the distribution of Xp11 translocation renal cell carcinomas in consecutively treated renal cell carcinomas in China.

TFE3 break-apart FISH assay is currently the gold standard for the diagnosis of Xp11 translocation renal cell carcinoma [23]. However, FISH analysis can't be performed in some departments of pathology, especially in some developing countries, and accordingly TFE3 immunohistochemistry analysis has been a powerful assistant for the diagnosis. In addition, it is difficult to detect the rearrangement caused by an inversion of chromosome X, such as *NONO-TFE3*, *RBM10-TFE3*, or *GRIPAP1-TFE3* gene fusion by *TFE3* break-apart FISH assay [11–13, 28]. In these cases, high TFE3 expression could be detected by immunohistochemistry staining, therefore, TFE3 immunohistochemistry staining is also a good screening method to decrease the false negative rate of FISH analysis. However, some studies have revealed that TFE3 immunohistochemistry could show false positive, false negative, and equivocal results due to differences in fixation times, technical methods and scoring system [20, 22–25]. In our study, we used the automated Ventana BenchMark XT system and all 20 cases of Xp11 translocation renal cell carcinomas were strong positive (3+) in nuclei with clean background and negative staining in paraneoplastic normal renal tubular epithelium. According to our scoring criteria, there was no case of diffusely mild to moderate or focally strong positive with 1+ or 2+ in all 20 cases of Xp11 translocation renal cell carcinomas. As a result, we think the automated Ventana BenchMark XT system may have better staining effect of TFE3 immunohistochemistry to reduce equivocal results, but it should be confirmed by further investigations because of the insufficiency of our number of cases.

In our study, the seven clear cell renal cell carcinomas with TFE3 strong positive immunostaining had the same histological features and immunoprofiles as typical clear cell renal cell carcinomas and were confirmed to be negative for *TFE3* break-apart by FISH. In addition, RNA sequencing showed that there was no *TFE3*-related gene fusion in these seven clear cell renal cell carcinomas, which further excluded the Xp11 translocation renal cell carcinomas with inversion of chromosome X such as *NONO*, *RBM10*, *GRIPAP1*, or unknown *TFE3*-related fusion partner. We think that the genetic alterations other than *TFE3* translocation may explain the presence of high TFE3 nuclear expression in very few clear cell renal cell carcinomas, which are similar to some reports in granular cell tumors and solid-pseudopapillary neoplasms of pancreas with

Table 2 Comparison of detailed morphologic findings between 20 Xp11 translocation renal cell carcinomas and seven clear cell renal cell carcinomas with strong positive immunostaining for TFE3

Histopathologic features	Xp11 TRCC	CCRCC	P^a
Alveolar, nested architecture	14 (70%)	7 (100%)	0.100
Solid architecture	4 (20%)	1 (14%)	0.738
Papillary architecture	10 (50%)	2 (29%)	0.326
Pseudopapillary architecture	0 (0%)	2 (29%)	**0.013**
Cystic architecture similar to multilocular cystic renal neoplasm of low malignant potential	1 (5%)	0 (0%)	0.547
High columnar cells and nuclei toward the luminal surface (secretory endometrioid)	1 (5%)	0 (0%)	0.547
Resembling collecting duct carcinoma architecture	1 (5%)	0 (0%)	0.547
Entrapped benign renal tubules	1 (5%)	0 (0%)	0.547
Trabecular architecture	1 (5%)	1 (14%)	0.419
Only clear cytoplasm	3 (15%)	2 (29%)	0.426
Only eosinophilic cytoplasm	3 (15%)	0 (0%)	0.277
Pale to eosinophilic flocullent cytoplasm	8 (40%)	0 (0%)	**0.046**
Clear and eosinophilic cytoplasm	6 (30%)	5 (71%)	0.055
Psammomatous calcification	10 (50%)	0 (0%)	**0.018**
Foamy histiocytes	5 (25%)	0 (0%)	0.143
Necrosis	4 (20%)	5 (71%)	**0.013**
Extreme nuclear pleomorphism	0 (0%)	2 (29%)	**0.013**
Rhabdoid differentiation	0 (0%)	1 (14%)	0.085
Cytoplasmic melanin pigment	2 (10%)	0 (0%)	0.385
Nuclear pseudoinclusions	1 (5%)	0 (0%)	0.547
Cytoplasmic vacuolization	1 (5%)	0 (0%)	0.547
Cytoplasmic eosinophilic granular bodies	1 (5%)	0 (0%)	0.547

Xp11 TRCC Xp11 translocation renal cell carcinoma, *CCRCC* clear cell renal cell carcinoma

[a]Chi-Square test

The bold values mean *P* value is less than 0.05

Table 3 Comparison of clinicopathological features between 20 Xp11 translocation renal cell carcinomas and seven clear cell renal cell carcinomas with strong positive immunostaining for TFE3

Clinical features	Xp11 TRCC	CCRCC	*P*
Mean age (years)	39.2	54.9	**0.018**[a]
Sex			0.098
Male	10	6	
Female	10	1	
Mean size (cm)	4.3	6.7	**0.026**[a]
Grade (ISUP)			**0.020**
Grade 1	1	0	
Grade 2	10	2	
Grade 3	9	2	
Grade 4	0	3	
Stage (pTNM)			0.226
pT1aNxMx	8	2	
pT1bNxMx	7	1	
pT2aNxMx	0	1	
pT3aN0/1/xMx or pT1bN1Mx	5	3	

Chi-Square tests for all the other analysis

Xp11 TRCC Xp11 translocation renal cell carcinoma, *CCRCC* clear cell renal cell carcinoma, *ISUP* International Society of Urological Pathology

[a]Independent Samples *t*-Test

The bold values mean *P* value is less than 0.05

Table 4 Comparison of immunohistochemistry findings between 20 Xp11 translocation renal cell carcinomas and 7 clear cell renal cell carcinomas with strong positive immunostaining for TFE3

IHC markers	Xp11 TRCC	CCRCC	P^a
CK7	Positive (3/20, 15%)	Positive (0/7, 0%)	0.277
CD117	Positive (1/20, 5%)	Positive (0/7, 0%)	0.547
CD10	Positive (13/20, 65%)	Positive (6/7, 86%)	0.302
P504s	Positive (19/20, 95%)	Positive (7/7, 100%)	0.547
Vimentin	Positive (10/20, 50%)	Positive (7/7, 100%)	**0.018**
CA-IX	Positive (2/20, 10%)	Positive (7/7, 100%)	**<0.001**
AE1/AE3	Positive (10/20, 50%)	Positive (7/7, 100%)	**0.018**
EMA	Positive (4/20, 20%)	Positive (5/7, 71%)	**0.013**
HMB45	Positive (2/20, 10%)	Positive (0/7, 0%)	0.385
Melan-A	Positive (3/20, 15%)	Positive (0/7, 0%)	0.277
CathepsinK	Positive (6/20, 30%)	Positive (0/7, 0%)	0.100

Xp11 TRCC Xp11 translocation renal cell carcinoma, *CCRCC* clear cell renal cell carcinoma, *IHC* immunohistochemistry

[a]Chi-Square test

The bold values mean *P* value is less than 0.05

immunohistochemistry-positive and FISH-negative results for TFE3 [29, 30]. As far as we know, this is the first time to report a very small minority (7/1604, 0.4%) of clear cell renal cell carcinomas with TFE3 strong positive immunostaining, which need to be future confirmed by *VHL* gene inactivation and more other studies. At the same time, our results illustrate a potential pitfall in diagnosis of Xp11 translocation renal cell carcinomas by TFE3 immunohistochemistry staining; that is to say, the strong positive staining of TFE3 is not specific for Xp11 translocation renal cell carcinomas because the clear cell renal cell carcinomas account for 26% (7/27) in our 27 cases of renal cell carcinomas with TFE3 strong positive immunostaining.

In order to find some useful information for the differential diagnosis, we compared the morphologic patterns, clinicopathological features, and immunoprofiles of the 20 Xp11 translocation renal cell carcinomas and seven clear cell renal cell carcinomas with TFE3 strong positive

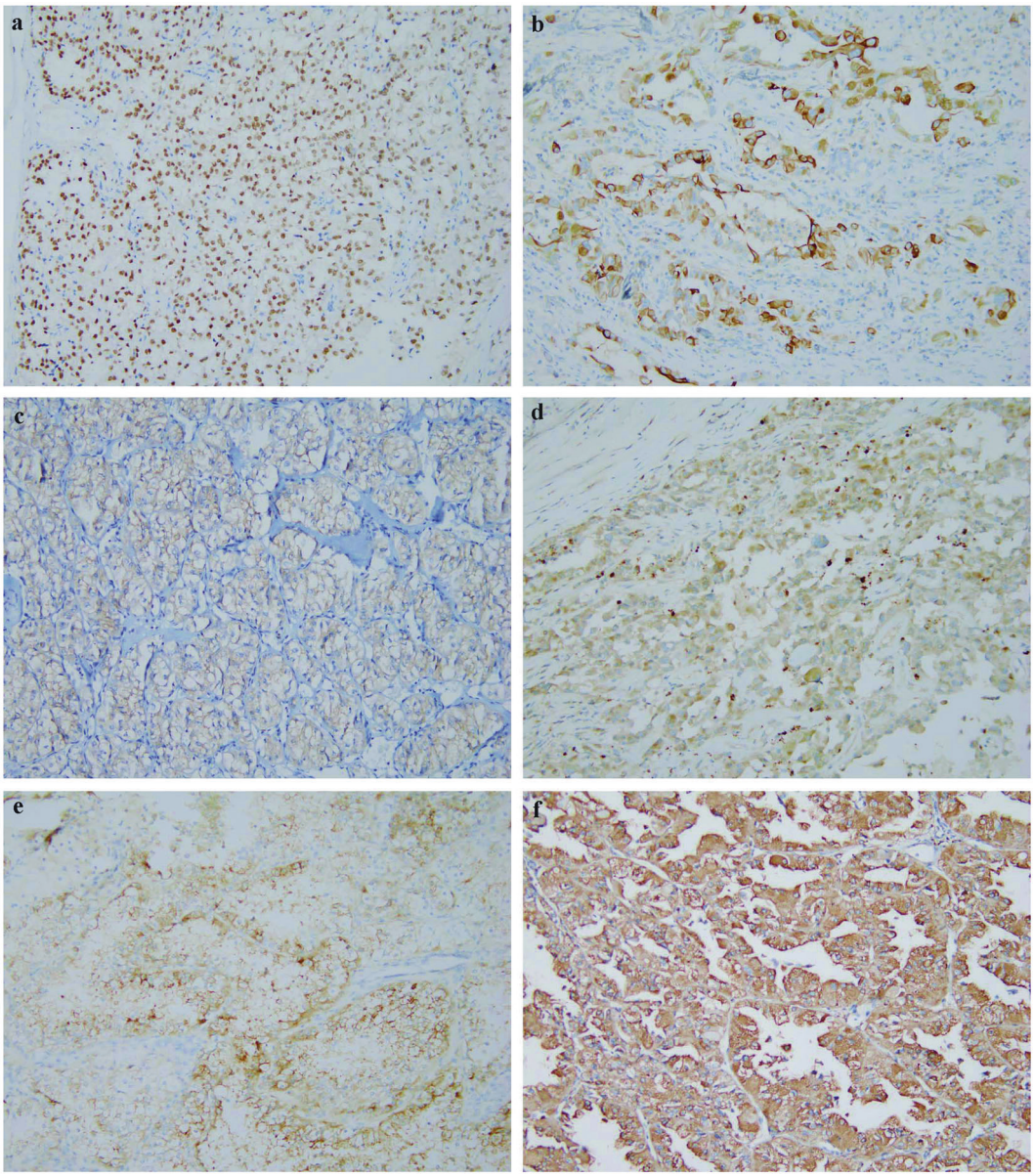

Fig. 5 Some immunohistochemical findings in Xp11 translocation renal cell carcinomas, including **a** strong positive (3+) staining for PAX8, ×200; **b** moderate positive (2+) staining for CK7, ×200; **c** moderate positive (2+) staining for CD117, ×200; **d** moderate positive (2+) staining for HMB45, ×200; **e** focally positive staining for Melan-A, ×200; **f** strong positive (3+) staining for CathepsinK, ×200

immunostaining. Through morphological comparison, we noticed that psammomatous calcification and pale to eosinophilic flocculent cytoplasm had statistical significance ($P < 0.05$) because they were seen only in Xp11 translocation renal cell carcinomas and had a higher frequency of occurrence (50% and 40%, respectively). Therefore, we think that their appearance has important value in differential diagnosis. Moreover, we also observed some histological features in our Xp11 translocation renal cell carcinomas, which have been reported in previous studies, such as the cystic architecture similar to multilocular cystic renal neoplasm of low malignant potential [31], high columnar cells and nuclei toward the luminal surface (secretory endometrioid) [3, 11], resembling collecting duct carcinoma architecture [19, 27], entrapped benign renal tubules [32], only eosinophilic cytoplasm [32], foamy histiocytes [20, 32], cytoplasmic melanin pigment [3, 13, 20], nuclear pseudoinclusions [19, 32], cytoplasmic vacuolization [13, 32], whereas they were not found in seven clear cell renal cell carcinomas. Although they appear less frequently in our cohort, their appearance may still provide diagnostic clues for Xp11 translocation renal cell carcinomas. On the other hand, pseudopapillary architecture and extreme nuclear pleomorphism were observed in clear cell

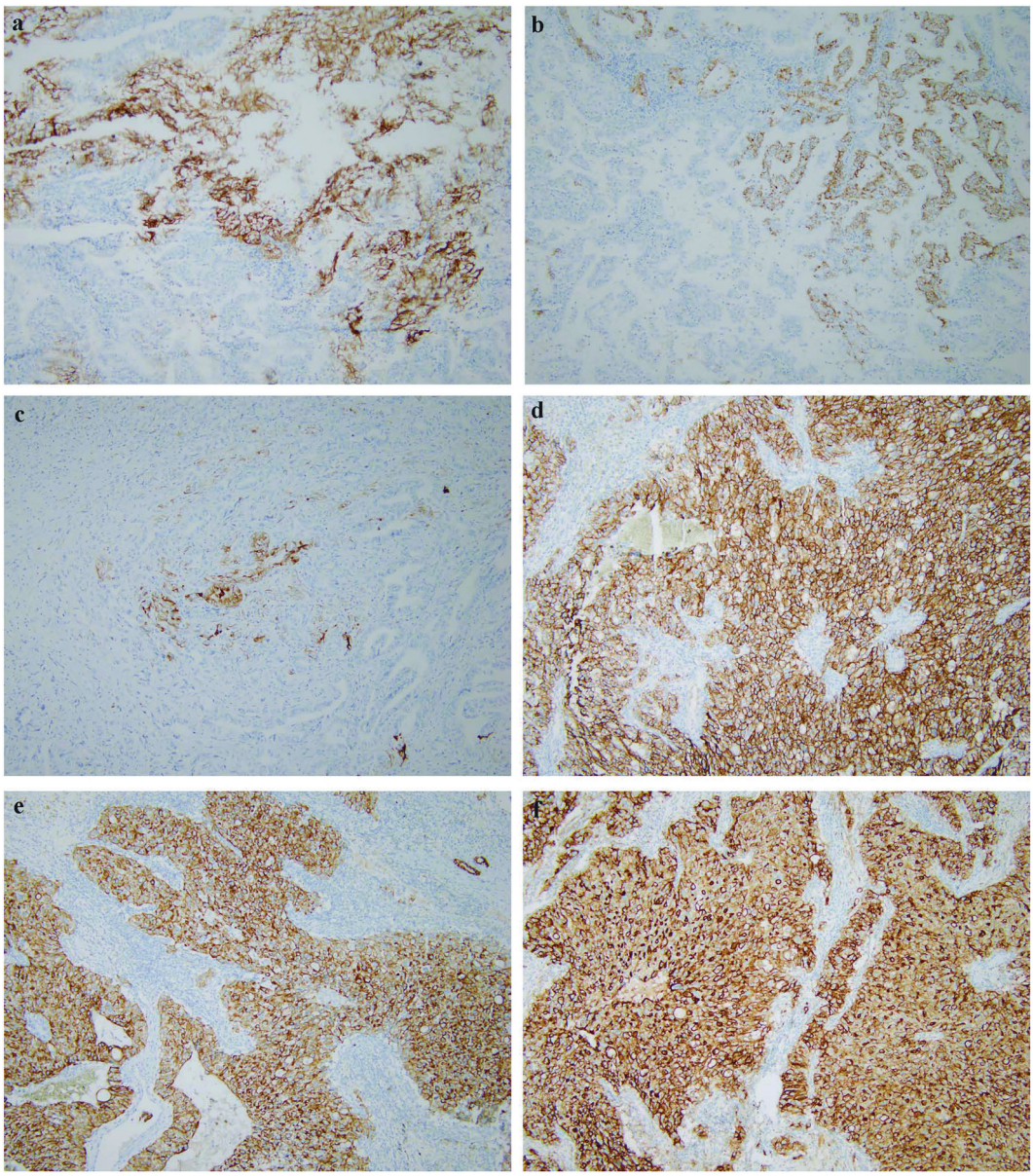

Fig. 6 Some different positive staining patterns for CA-IX, AE1/AE3 and EMA between Xp11 translocation renal cell carcinomas and clear cell renal cell carcinomas, such as focally positive staining in Xp11 translocation renal cell carcinomas for **a** CA-IX, **b** AE1/AE3, and **c** EMA, ×100; and diffusely strong positive staining in clear cell renal cell carcinomas for **d** CA-IX, **e** AE1/AE3, and **f** EMA, ×100

renal cell carcinomas, but not in 20 Xp11 translocation renal cell carcinomas ($P < 0.05$). Argani et al [8] observed pseudopapillary architecture in *ASPL-TFE3* renal cell carcinomas, and Skala et al [32] recently reported four cases of Xp11 translocation renal cell carcinomas with predominant pseudopapillary architecture without specific information about fusion partners. We didn't find pseudopapillary architecture in our 20 Xp11 translocation renal cell carcinomas but found it in two cases of clear cell renal cell carcinomas, which suggests that pseudopapillary structure is not unique to Xp11 translocation renal cell carcinomas, but probably is the secondary change caused by tumor necrosis. Interestingly, we found a case of Xp11 translocation renal cell carcinomas with cytoplasmic eosinophilic granular bodies, to our knowledge, which has not been reported in the previous literature.

Our study showed that compared with seven clear cell renal cell carcinomas, Xp11 translocation renal cell carcinomas were more frequent in younger patients with smaller tumor size and lower WHO/ISUP grade. Moreover, in our 20 Xp11 translocation renal cell carcinomas, we did not observe any grade four features, which have been reported in Xp11 translocation renal cell carcinomas including nuclear pleomorphism [22], tumour giant cells [9, 27],

rhabdoid [20], and sarcomatoid differentiation [3, 27, 32]. Tumor necrosis was observed in all Xp11 translocation renal cell carcinomas with pT3a stage, but not found in other Xp11 translocation renal cell carcinomas at earlier stage. Accordingly, we think tumor necrosis could be an important clue to hint pT3a stage in Xp11 translocation renal cell carcinoma, since it is often accompanied with some features of pT3a stage including tumor cells invasion into renal vein or its segmental branches, perirenal fat, renal sinus fat, and pelvis. In our study, all four patients of Xp11 translocation renal cell carcinomas in pT3a stage had local recurrence and distant metastasis, and even two of them died, within 3 years. Sukov et al [6] reported that one of six cases of Xp11 translocation renal cell carcinomas was pT3a stage, and the patient died 0.8 year after operation. Therefore, we think that pT3a stage may be a high-risk factor for Xp11 translocation renal cell carcinomas, which needs to be validated by multi-institutional studies. In addition, our data indicated there was no significant difference in prognosis between Xp11 translocation renal cell carcinoma and clear cell renal cell carcinoma with TFE3 strong positive immunostaining, but more cases and longer follow-up time need to support this result because of the insufficiency of our number of cases and follow-up time.

As we know, a panel of immunohistochemistry markers is useful to classify the subtypes of renal cell carcinomas. Our results showed that Vimentin, CA-IX, AE1/AE3, and EMA were most frequently positive in clear cell renal cell carcinomas with diffusely strong staining, but often focally mild or moderate positive (even negative) in Xp11 translocation renal cell carcinomas. Among them, CA-IX is the best marker for the differential diagnosis. Argani et al [33] reported that CA-IX was focal staining (mean 5.7% tumor cells) in Xp11 translocation renal cell carcinomas while diffuse staining (100% tumor cells) in clear cell renal cell carcinomas, which was consistent with our results. We also performed immunohistochemistry for melanocytic markers (HMB45, Melan-A, and CathepsinK) to differentiate Xp11 translocation renal cell carcinomas and melanotic Xp11 translocation renal cancers, which were reported to be positive for melanocytic markers and negative for PAX8 [3, 34]. The positive rates of HMB45, Melan-A and CathepsinK were 10%, 15%, and 30% in our Xp11 translocation renal cell carcinomas, respectively. Both HMB45 and Melan-A were usually focal positive (except case 20), whereas CathepsinK was diffuse positive. One Xp11 translocation renal cell carcinoma (case 20) was diffusely strong positive for Melan-A and CathepsinK with architecture similar to multilocular cystic renal neoplasm of low malignant potential, which is consistent with *MED15-TFE3* renal cell carcinomas reported by Wang et al [19]. In addition, another Xp11 translocation renal cell carcinoma (case 5) showed diffusely moderate positive for CD117 and focally moderate positive for CK7, and the morphology displayed alveolar or nested architecture by hyalinized and calcified vascular septa with pale to eosinophilic flocculent cytoplasm without psammomatous calcification. If TFE3 immunohistochemistry was not done, it could be misdiagnosed as chromophobe renal cell carcinoma or oncocytoma.

In summary, based on the immunohistochemistry staining for TFE3 in large-scale consecutively treated renal cell carcinomas, we first demonstrate that the strong positive immunostaining of TFE3 is not absolutely unique for Xp11 translocation renal cell carcinomas, but also occurs in a very small minority (0.4%) of clear cell renal cell carcinomas, which points out a potential pitfall in diagnosis of Xp11 translocation renal cell carcinomas by TFE3 immunohistochemistry. Tumor necrosis could be a potential factor relevant to pT3a stage, which may be a high-risk factor for the patients with Xp11 translocation renal cell carcinomas. We report the first case of Xp11 translocation renal cell carcinoma with cytoplasmic eosinophilic granular bodies. Our study highlights that CA-IX is a good marker for differential diagnosis of Xp11 translocation renal cell carcinomas and clear cell renal cell carcinomas with TFE3 strong positive immunostaining.

Acknowledgements This work was supported by grants from the National Natural Science Foundation of China (81472391 and 81871990 to Y.S, and 81572851 to Y.M).

Compliance with ethical standards

Conflict of interest The authors declare that they have no conflict of interest.

References

1. Argani P, Ladanyi M. Renal carcinomas associated with Xp11.2 translocations/TFE3 gene fusions. In: Eble JN, Sauter G, Epstein JI, Sesterhenn IA, editors. Pathology and Genetics of Tumours of the Urinary System and Male Genital Organs. Lyon; IARC Press; 2004. p. 37–8.
2. Argani P, Cheville J, Ladanyi M. MiT family translocation renal cell carcinomas. In: Moch H, Humphrey PA, Ulbright TM, Reuter VE, editors. WHO Classification of Tumours of the Urinary System and Male Genital Organs. Lyon: IARC Press; 2016. p. 33–4.
3. Argani P, Zhong M, Reuter VE, Fallon JT, Epstein JI, Netto GJ, et al. TFE3-fusion variant analysis defines specific clinicopathologic associations among Xp11 translocation cancers. Am J Surg Pathol. 2016;40:723–37.
4. Ramphal R, Pappo A, Zielenska M, Grant R, Ngan BY. Pediatric renal cell carcinoma: clinical, pathologic, and molecular abnormalities associated with the members of the mit transcription factor family. Am J Clin Pathol. 2006;126:349–64.

5. Komai Y, Fujiwara M, Fujii Y, Mukai H, Yonese J, Kawakami S, et al. Adult Xp11 translocation renal cell carcinoma diagnosed by cytogenetics and immunohistochemistry. Clin Cancer Res. 2009;15:1170–6.
6. Sukov WR, Hodge JC, Lohse CM, Leibovich BC, Thompson RH, Pearce KE, et al. TFE3 rearrangements in adult renal cell carcinoma: clinical and pathologic features with outcome in a large series of consecutively treated patients. Am J Surg Pathol. 2012;36:663–70.
7. Ellis CL, Eble JN, Subhawong AP, Martignoni G, Zhong M, Ladanyi M, et al. Clinical heterogeneity of Xp11 translocation renal cell carcinoma: impact of fusion subtype, age and stage. Mod Pathol. 2014;27:875–86.
8. Argani P, Antonescu CR, Illei PB, Lui MY, Timmons CF, Newbury R, et al. Primary renal neoplasms with the ASPL-TFE3 gene fusion of alveolar soft part sarcoma: a distinctive tumor entity previously included among renal cell carcinomas of children and adolescents. Am J Pathol. 2001;159:179–92.
9. Argani P, Antonescu CR, Couturier J, Fournet JC, Sciot R, Debiec-Rychter M, et al. PRCC-TFE3 renal carcinomas: morphologic, immunohistochemical, ultrastructural, and molecular analysis of an entity associated with the t(X;1)(p11.2; q21). Am J Surg Pathol. 2002;26:1553–66.
10. Clark J, Lu YJ, Sidhar SK, Parker C, Gill S, Smedley D, et al. Fusion of splicing factor genes PSF and NonO (p54nrb) to the TFE3 gene in papillary renal cell carcinoma. Oncogene. 1997;15:2233–9.
11. Xia QY, Wang Z, Chen N, Gan HL, Teng XD, Shi SS, et al. Xp11.2 translocation renal cell carcinoma with NONO-TFE3 gene fusion: morphology, prognosis, and potential pitfall in detecting TFE3 gene rearrangement. Mod Pathol. 2017;30:416–26.
12. Argani P, Zhang L, Reuter VE, Tickoo SK, Antonescu CR. RBM10-TFE3 renal cell carcinoma: a potential diagnostic pitfall due to cryptic intrachromosomal Xp11.2 inversion resulting in false-negative TFE3 FISH. Am J Surg Pathol. 2017;41:655–62.
13. Xia QY, Wang XT, Zhan XM, Tan X, Chen H, Liu Y, et al. Xp11 translocation renal cell carcinomas (RCCs) with RBM10-TFE3 gene fusion demonstrating melanotic features and overlapping morphology with t(6;11) RCC: interest and diagnostic pitfall in detecting a paracentric inversion of TFE3. Am J Surg Pathol. 2017;41:663–76.
14. Argani P, Lui MY, Couturier J, Bouvier R, Fournet JC, Ladanyi M. A novel CLTC-TFE3 gene fusion in pediatric renal adenocarcinoma with t(X;17)(p11.2; q23). Oncogene. 2003;22:5374–8.
15. Huang W, Goldfischer M, Babyeva S, Mao Y, Volyanskyy K, Dimitrova N, et al. Identification of a novel PARP14-TFE3 gene fusion from 10-year-old FFPE tissue by RNA-seq. Genes Chromosomes Cancer. 2015;54:500–5.
16. Malouf GG, Su X, Yao H, Gao J, Xiong L, He Q, et al. Next-generation sequencing of translocation renal cell carcinoma reveals novel RNA splicing partners and frequent mutations of chromatin-remodeling genes. Clin Cancer Res. 2014;20:4129–40.
17. Classe M, Malouf GG, Su X, Yao H, Thompson EJ, Doss DJ, et al. Incidence, clinicopathological features and fusion transcript landscape of translocation renal cell carcinomas. Histopathology. 2017;70:1089–97.
18. Antic T, Taxy JB, Alikhan M, Segal J. Melanotic translocation renal cell carcinoma with a novel ARID1B-TFE3 gene fusion. Am J Surg Pathol. 2017;41:1576–80.
19. Wang XT, Xia QY, Ye SB, Wang X, Li R, Fang R, et al. RNA sequencing of Xp11 translocation-associated cancers reveals novel gene fusions and distinctive clinicopathologic correlations. Mod Pathol. 2018;31:1346–60.
20. Rao Q, Williamson SR, Zhang S, Eble JN, Grignon DJ, Wang M, et al. TFE3 break-apart FISH has a higher sensitivity for Xp11.2 translocationassociated renal cell carcinoma compared with TFE3 or cathepsinK immunohistochemical staining alone: expanding the morphologic spectrum. Am J Surg Pathol. 2013;37:804–15.
21. Argani P, Lal P, Hutchinson B, Lui MY, Reuter VE, Ladanyi M. Aberrant nuclear immunoreactivity for TFE3 in neoplasms with TFE3 gene fusions: a sensitive and specific immunohistochemical assay. Am J Surg Pathol. 2003;27:750–61.
22. Argani P, Aulmann S, Illei PB, Netto GJ, Ro J, Cho HY, et al. A distinctive subset of PEComas harbors TFE3 gene fusions. Am J Surg Pathol. 2010;34:1395–406.
23. Camparo P, Vasiliu V, Molinie V, Couturier J, Dykema KJ, Petillo D, et al. Renal translocation carcinomas: clinicopathologic, immunohistochemical, and gene expression profiling analysis of 31 cases with a review of the literature. Am J Surg Pathol. 2008;32:656–70.
24. Mosquera JM, Dal Cin P, Mertz KD, Perner S, Davis IJ, Fisher DE, et al. Validation of a TFE3 break-apart FISH assay for Xp11.2 translocation renal cell carcinomas. Diagn Mol Pathol. 2011;20:129–37.
25. Green WM, Yonescu R, Morsberger L, Morris K, Netto GJ, Epstein JI, et al. Utilization of a TFE3 breakapart FISH assay in a renal tumor consultation service. Am J Surg Pathol. 2013;37:1150–63.
26. Sun BC, Sun Y, Wang J, Zhao X, Zhang S, Liu Y, et al. The diagnostic value of SYT-SSX detected by RT-PCR and FISH for synovial sarcoma: a review and Prospective study of 255 cases. Cancer Sci. 2008;99:1355–61.
27. Argani P, Olgac S, Tickoo SK, Goldfischer M, Moch H, Chan DY, et al. Xp11 translocation renal cell carcinoma in adults: expanded clinical, pathologic, and genetic spectrum. Am J Surg Pathol. 2007;31:1149–60.
28. Wang XT, Xia QY, Zhou XJ, Rao Q. Incidence, clinicopathological features and fusion transcript landscape of translocation renal cell carcinomas. Histopathology. 2017;71:835–6.
29. Schoolmeester JK, Lastra RR. Granular cell tumors overexpress TFE3 without corollary gene rearrangement. Hum Pathol. 2015;46:1242–3.
30. Harrison G, Hemmerich A, Guy C, Perkinson K, Fleming D, McCall S, et al. Overexpression of sox11 and tfe3 in solid-pseudopapillary neoplasms of the pancreas. Am J Clin Pathol. 2017;149:67–75.
31. Suzigan S, Drut R, Faria P, Argani P, De Marzo AM, Barbosa RN, et al. Xp11 translocation carcinoma of the kidney presenting with multilocular cystic renal cell carcinomalike features. Int J Surg Pathol. 2007;15:199–203.
32. Skala SL, Xiao H, Udager AM, Dhanasekaran SM, Shukla S, Zhang Y, et al. Detection of 6 TFEB-amplified renal cell carcinomas and 25 renal cell carcinomas with MITF translocations: systematic morphologic analysis of 85 cases evaluated by clinical TFE3 and TFEB FISH assays. Mod Pathol. 2018;31:179–97.
33. Argani P, Hicks J, De Marzo AM, Albadine R, Illei PB, Ladanyi M, et al. Xp11 translocation renal cell carcinoma (RCC): extended immunohistochemical profile emphasizing novel RCC markers. Am J Surg Pathol. 2010;34:1295–303.
34. Rao Q, Shen Q, Xia QY, Wang ZY, Liu B, Shi SS, et al. PSF/SFPQ is a very common gene fusion partner in TFE3 rearrangement-associated perivascular epithelioid cell tumors (PEComas) and melanotic Xp11 translocation renal cancers: clinicopathologic, immunohistochemical, and molecular characteristics suggesting classification as a distinct entity. Am J Surg Pathol. 2015;39:1181–96.